J|A|C|S COMMUNICATIONS

Published on Web 02/06/2009

Synthesis of Stishovite Nanocrystals from Periodic Mesoporous Silica

Paritosh Mohanty,† Dong Li,† Tianbo Liu,† Yingwei Fei,‡ and Kai Landskron*,†

Department of Chemistry, Lehigh University, Bethlehem, Pennsylvania 18015, and Geophysical Laboratory, Carnegie Institution of Washington, Washington, D.C. 20015

Received September 21, 2008; E-mail: kal205@lehigh.edu

Stishovite, a high-pressure polymorph of silica, was first synthesized in the laboratory[1] and later observed in shocked specimens from terrestrial impact structures.[2] This is one of the hardest oxidic materials, with a hardness of 33 GPa,[3] and is believed to be secondary to cotunnite-type TiO_2, which was synthesized at 60 GPa, a much higher pressure than the ~10 GPa for stishovite.[4] Recently, anisotropic hardness was observed for single-crystalline stishovite.[5] Its hardness was reported as 31.8 ± 1.0 GPa along the *c* axis and 26.2 ± 1.0 GPa along a perpendicular direction.[5] Diamond is the hardest known material and is used in many modern-day applications, such as tool grinding, rock drilling, concrete cutting, stone polishing, machining, and so on. However, its reactions with iron and silicon restrict its use in some applications, such as machining steel. Therefore, alternatives to diamond are sought. According to the Hall−Petch relation, the yield stress of a crystalline material is inversely proportional to the square root of the grain size. Thus, there are intense efforts directed toward the synthesis of high-strength nanocrystalline materials.[6]

Few reports on the synthesis of stishovite are available, and all of these are confined to bulk specimens.[1,5,7−13] Recently, the stability and phase transition of stishovite were also studied theoretically.[14−16] To the best of our knowledge, no report on the synthesis of stishovite nanostructures is available. In this communication, we report the synthesis of stishovite nanocrystals from periodic mesoporous silicas by a high-pressure experiment using a multianvil apparatus. Because of their relatively facile synthesis, they could be potentially used as a hard material in, for example, cutting and polishing applications.

Mesoporous silica SBA-16, with $Im\bar{3}m$ body-centered cubic symmetry, was used as the precursor for the synthesis of stishovite nanocrystals. The SBA-16 was synthesized according to the reported procedure.[17] The high-pressure behavior of periodic mesoporous silica was previously investigated by Tolbert and co-workers,[18] but the investigations were restricted to room temperature. In a typical stishovite synthesis, ~20 mg of SBA-16 was placed in a Pt capsule and heated in a Re furnace. The pressure of the system was increased to 12 GPa at a rate of 1−2 GPa/h. After the pressure of the system reached the desired value of 12 GPa, the temperature was raised to 400 °C at a heating rate of ~100 °C/min, after which the system was kept at that temperature for 5 min and then quenched to room temperature.

The synthesis of stishovite from the SBA-16 precursor resulted in the formation of faceted nanocrystals, as revealed by scanning electron microscopy (SEM) and transmission electron microscopy (TEM) images of the product (Figure 1). The average particle size was measured to be between 200 and 400 nm. The particles have faceted polygonal shapes, as shown in the SEM image. The nanocrystals are not sintered together according to SEM. The selected-area electron diffraction (SAED) pattern (inset of Figure 1b) shows bright, regular arrays of diffraction spots, indicating that the individual nanoparticles are single-crystalline. The average particle size of the nanocrystals was further studied with dynamic light scattering (DLS) measurements. Here the nanocrystals were dispersed in water, and the hydrodynamic radius (R_h) was measured at different scattering angles (from 90 to 30°) using DLS and analyzed by the CONTIN method (Figure 2). The R_{h0} value can be calculated by extrapolating R_h to 0° (Figure S1 in the Supporting Information). The average particle diameter of the nanocrystals calculated from the DLS study was 282 ± 16 nm with a polydispersity of 1.25. This value further supports the TEM and SEM results. Furthermore, it indicates that the nanocrystals are not agglomerated but remain suspended as individual nanocrystals in aqueous media. The weak angular dependence of the R_h values suggests that the suspended particles are in general isotropic in shape. We also studied the energy-dispersive spectroscopy (EDS) spectrum of the specimen (Figure S2). It shows only Si and O, confirming the SiO_2 composition and the absence of impurities.

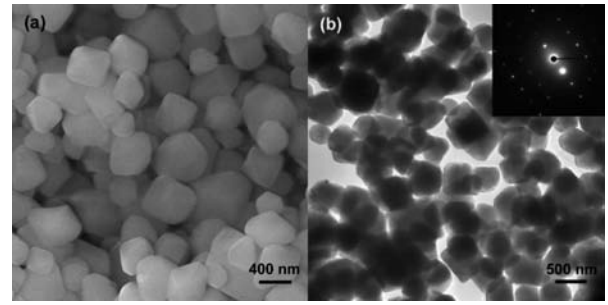

Figure 1. (a) SEM and (b) TEM images of stishovite nanocrystals. The SAED pattern is given in the inset of (b).

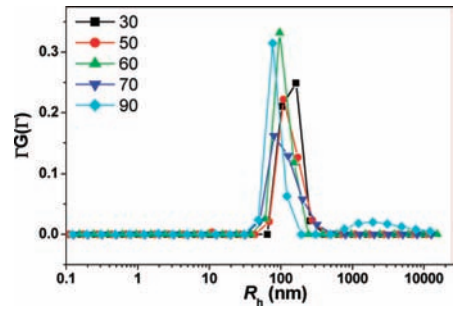

Figure 2. Hydrodynamic radii (R_h) distributions of stishovite nanocrystals, obtained by CONTIN analysis of the DLS measurements at various scattering angles between 30 and 90°.

The phase of the obtained specimen was confirmed by X-ray diffraction (XRD). Figure 3 shows a typical XRD pattern of the specimen. All of the observed reflections in the diffractogram are

† Lehigh University.
‡ Carnegie Institution of Washington.

10.1021/ja8075007 CCC: $40.75

unambiguously indexed to the $P4_2/mnm$ tetragonal crystal structure of stishovite (JCPDS file 45-1374). The lattice parameters were refined to be $a = 0.4186$ nm and $c = 0.2669$ nm, which are comparable to the standard values of $a = 0.4179$ nm and $c = 0.2666$ nm.

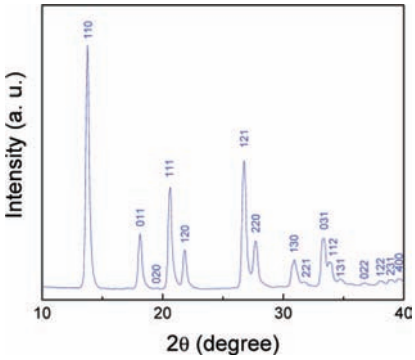

Figure 3. XRD pattern of stishovite nanocrystals.

The structure of the specimen was confirmed by Raman spectroscopy. The Raman spectrum of the stishovite shown in Figure S3a in the Supporting Information was characterized by well-resolved bands at 232, 590, 755, and 967 cm^{-1}, which are assigned to the B_{1g}, E_g, A_{1g}, and B_{2g} fundamental vibrational modes, respectively. Similar bands were also observed for both synthetic and natural bulk stishovite.[11,19] These bands are characteristic of rutile-structured oxides.[20] The specimen was further studied using FT-IR spectroscopy (Figure S3b). Six bands were observed, at 557, 613, 648, 840, 870, and 932 cm^{-1}. They can be assigned to the E_u and A_{2u} vibrational modes.[21,22] The positions of the bands deviate from those of reported synthetic and natural stishovite[21,22] because band positions in rutile-structured compounds principally depend on particle size and geometry.[23] No band was observed in the 2500−4000 cm^{-1} region. This indicates that the sample was free of silanol groups within the detection limits of IR spectroscopy.

In an attempt to understand the effect of the pore structure on the synthesis of the stishovite nanocrystals, we performed an analogous experiment using as the precursor mesoporous silica KIT-6, which has *Ia3d* cubic symmetry (the gyroid structure). Faceted single-crystalline stishovite nanocrystals with larger sizes (400−800 nm) than those of the nanocrystals obtained from SBA-16 (200−400 nm) were observed (Figures S4−S6 in the Supporting Information). Furthermore, we investigated the behavior of SBA-15, which has a hexagonal honeycomb structure with one-dimensional mesochannels. Surprisingly, in this case we obtained coesite according to XRD (Figure S7). According to TEM (Figure S8) and SEM (Figure S9), no well-defined morphology was observed. We conclude that the kinetic pathway of the reaction plays a major role in the product formation. Apparently, in the case of the cubic mesostructures SBA-16 and KIT-6, a direct pathway to stishovite on the free-energy surface is favored, while in the case of SBA-15, a pathway through coesite as an intermediate is favored. Because of the low reaction temperature of 400 °C, the coesite intermediate is stable enough that it does not convert further to form stishovite at a significant rate. This raises the question of why the kinetic pathway is impacted by the different mesostructures. Tolbert and co-workers[18b] have shown that pressure-induced Si−O−Si intertetrahedral bond angle increase is suppressed by the presence of hexagonal mesoporosity in silicas, which disfavors denser structures at the atomic scale. Instead, compression occurs at the mesoscale.[18b] These pressure-induced bond-angle changes and thus densities at the atomic scale should be greater for cubic mesostructures because of their higher mechanical stabilities.[24] The cubic mesostructures that experience higher compression at the atomic scale tend to favor a direct pathway to the denser stishovite, while in the mechanically weaker hexagonal SBA-15, the opposite is the case and thus a kinetic route to coesite is favored.

Acknowledgment. We gratefully acknowledge financial support from Lehigh University. We thank Liwei Deng, Yao Wu, Li Zhang, and Dr. Alexander Goncharov for technical assistance.

Supporting Information Available: Experimental procedures and Figures S1−S9. This material is available free of charge via the Internet at http://pubs.acs.org.

References

(1) Stishov, S. M.; Popova, S. V. *Geokhimiya* **1961**, *10*, 837.
(2) Chao, E. C. T.; Fahey, J. J.; Littler, J.; Milton, D. J. *J. Geophys. Res.* **1962**, *67*, 419.
(3) Leger, J. M.; Haines, J.; Schmidt, M.; Petitet, J. P.; Pereira, A. S.; da Jornada, J. A. H. *Nature* **1996**, *383*, 401.
(4) Dubrovinsky, L. S.; Dubrovinskaia, N. A.; Swamy, V.; Muscat, J.; Harrison, N. M.; Ahuja, R.; Holm, B.; Johansson, B. *Nature* **2001**, *410*, 653.
(5) Luo, S. N.; Swadener, J. G.; Ma, C.; Tschauner, O. *Phys. B* **2007**, *399*, 138.
(6) (a) Pecharromán, C.; Esteban-Betegón, F.; Bartolomé, J. F.; Richter, G.; Moya, J. S. *Nano Lett.* **2004**, *4*, 747. (b) Shan, Z. W.; Adesso, G.; Cabot, A.; Sherburne, M. P.; Asif, S. A. S.; Warren, O. L.; Chrzan, D. C.; Minor, A. M.; Alivisatos, A. P. *Nat. Mater.* **2008**, *7*, 947. (c) Shen, X.; Lian, J.; Jiang, Z.; Jiang, Q. *Adv. Eng. Mater.* **2008**, *10*, 539.
(7) Wentorf, R. H. *J. Geophys. Res.* **1962**, *67*, 3648.
(8) Endo, S.; Akai, T.; Akahama, Y.; Wakatsuki, M.; Nakamura, T.; Tomii, Y.; Koto, K.; Ito, Y.; Tokonami, M. *Phys. Chem. Miner.* **1986**, *13*, 146.
(9) Li, B.; Rigden, S. M.; Liebermann, R. C. *Phys. Earth Planet. Inter.* **1996**, *96*, 113.
(10) Cordier, P.; Sharp, T. G. *Phys. Chem. Miner.* **1998**, *25*, 548.
(11) Hemley, R. J.; Mao, H. K.; Chao, E. C. T. *Phys. Chem. Miner.* **1986**, *13*, 285.
(12) Andrault, D.; Fiquet, G.; Guyot, F.; Hanfland, M. *Science* **1998**, *282*, 720.
(13) Texier, M.; Cordier, P. *Phys. Chem. Miner.* **2006**, *33*, 394.
(14) Tjabane, M.; Lowther, J. E. *Phys. B* **1999**, *270*, 164.
(15) Liang, Y.; Miranda, C. R.; Scandolo, S. *J. Chem. Phys.* **2006**, *125*, 194524.
(16) Luoa, S. N.; Zheng, L.; Tschauner, O. *Solid State Commun.* **2005**, *136*, 71.
(17) (a) Kim, T. W.; Ryoo, R.; Kruk, M.; Gierszal, K.; Jaroniec, M.; Kamiya, S.; Terasaki, O. *J. Phys. Chem. B* **2004**, *108*, 11480. (b) Kim, T. W.; Ryoo, R.; Gierszal, K. P.; Jaroniec, M.; Solovyov, L. A.; Sakamoto, Y.; Terasaki, O. *J. Mater. Chem.* **2005**, *15*, 1560. (c) Kleitz, F.; Kim, T. W.; Ryoo, R. *Langmuir* **2006**, *22*, 440. (d) Zhao, D.; Feng, J.; Huo, Q.; Melosh, N.; Fredrickson, G. H.; Chmelka, B. F.; Stucky, G. D. *Science* **1998**, *279*, 548.
(18) (a) Wu, J.; Liu, X.; Tolbert, S. H. *J. Phys. Chem. B* **2000**, *104*, 11837. (b) Wu, J.; Zhao, L.; Chronister, E. L.; Tolbert, S. H. *J. Phys. Chem. B* **2002**, *106*, 5613. (c) Lapen, A. M.; Wu, J.; Gross, A. F.; Tolbert, S. H. *J. Phys. Chem. B* **2002**, *106*, 11720.
(19) Gillet, P.; Cleach, A. L.; Madon, M. *J. Geophys. Res* **1990**, *95*, 21635.
(20) (a) Scott, J. F. *Phys. Rev. B* **1970**, *1*, 3488. (b) Sharma, S. K.; Virgo, D.; Kushiro, I. *J. Non-Cryst. Solids* **1979**, *33*, 235. (c) Beattie, I. R.; Gilson, T. R. *Proc. R. Soc. London, Ser. A* **1968**, *307*, 407. (d) Beattie, I. R.; Gilson, T. R. *J. Chem. Soc. A* **1969**, *1969*, 2322. (e) Peercy, P. S.; Morosin, B. *Phys. Rev. B* **1973**, *7*, 2779. (f) Porto, S. P. S.; Fleury, P. A.; Damen, T. C. *Phys. Rev.* **1967**, *154*, 522.
(21) Hofmeister, A. M.; Xu, J.; Akimoto, S. *Am. Mineral.* **1990**, *75*, 951.
(22) Williams, Q.; Hemley, R. J.; Kruger, M. B.; Jeanloz, R. *J. Geophys. Res.* **1993**, *98*, 22157.
(23) Luxon, J. T.; Summitt, R. *J. Chem. Phys.* **1969**, *50*, 1366.
(24) (a) Hartmann, M.; Vinu, A. *Stud. Surf. Sci. Catal.* **2003**, *146*, 285. (b) Fan, H.; Hartshorn, C.; Buchheit, T.; Tallant, D.; Assink, R.; Simpson, R.; Kissel, D. J.; Lacks, D. J.; Torquato, S.; Brinker, C. J. *Nat. Mater.* **2007**, *6*, 418.

JA8075007